Skeletal Radiology (2023) 52:349–363
https://doi.org/10.1007/s00256-022-04158-7

REVIEW ARTICLE

Imaging of spinal chordoma and benign notochordal cell tumor (BNCT) with radiologic pathologic correlation

Mark D. Murphey[1,2,3] · Matthew J. Minn[1,3,4] · Alejandro Luiña Contreras[5] · Kelly K. Koeller[1,6] · Robert Y. Shih[1,2,3] · Carrie Y. Inwards[7] · Takehiko Yamaguchi[8]

Received: 5 May 2022 / Revised: 27 July 2022 / Accepted: 29 July 2022 / Published online: 5 September 2022

Abstract

Benign notochordal cell tumor (BNCT) and chordoma are neoplasms of notochordal differentiation. BNCT represents notochordal rests, commonly an incidental lesion present in the spine in 19% of cadaveric specimens. BNCTs are often radiographically occult. CT of BNCT frequently reveals patchy sclerosis between areas of maintained underlying trabeculae. BNCT demonstrates marrow replacement on T1-weighted MR images with high signal intensity on T2-weighting. BNCTs are frequently smaller than 35 mm and lack significant enhancement, bone destruction, cortical permeation, or soft tissue components. Biopsy or surgical resection of BNCT is usually not warranted, although imaging surveillance may be indicated. Chordoma is a rare low-grade locally aggressive malignancy representing 1–4% of primary malignant bone tumors. Chordoma is most frequent between the ages of 50–60 years with a male predilection. Clinical symptoms, while nonspecific and location dependent, include back pain, numbness, myelopathy, and bowel/bladder incontinence. Unfortunately, lesions are often large at presentation owing to diagnosis delay. Imaging of chordoma shows variable mixtures of bone destruction and sclerosis, calcification (50–70% at CT) and large soft tissue components. MR imaging of chordoma reveals multilobulated areas of marrow replacement on T1-weighting and high signal intensity on T2-weighting reflecting the myxoid component within the lesion and areas of hemorrhage seen histologically. Treatment of chordoma is primarily surgical with prognosis related to resection extent. Unfortunately, complete resection is often not possible (21–75%) resulting in high local recurrence incidence (19–75%) and a 5-year survival rate of 45–86%. This article reviews and illustrates the clinical characteristics, pathologic features, imaging appearance spectrum, treatment, and prognosis of BNCT and spinal chordoma.

Keywords Benign notochordal cell tumor · Chordoma · WHO classification

The opinions and assertions contained herein are the private views of the authors and are not to be construed as official or as representing the views of the ACR Institute for Radiologic Pathology, nor the Departments of the Army, Navy, Air Force, or Defense.

✉ Mark D. Murphey
mmurphey@acr.org

[1] Musculoskeletal Imaging and Neuroradiology, ACR Institute for Radiologic Pathology (AIRP), 1100 Wayne Avenue, Suite 1020, Silver Spring, MD 20910, USA

[2] Uniformed Services University of the Health Sciences, 4301 Jones Bridge Road, Bethesda, MD 20814, USA

[3] Department of Radiology, Walter Reed National Military Medical Center, 8901 Wisconsin Ave., Bethesda, MD 20889, USA

[4] Department of Radiology, Scripps Green Hospital, 10666 N. Torrey Pines Road, La Jolla, CA 92037, USA

[5] Joint Pathology Center, 606 Stephen Sitter Avenue, Silver Spring, MD 20910-1290, USA

[6] Department of Radiology, Head and Neck Cancer Center, Mayo Clinic, 200 First Street SW, Rochester, MN 55905, USA

[7] Department of Laboratory Medicine and Pathology, Mayo Clinic, 200 First Street SW, Rochester, MN 55905, USA

[8] Department of Pathology, Nikko Medical Center, Dokkyo Medical University, 632 Takatoku, Nikko, Tochigi 321-2593, Japan

Introduction

The fifth edition WHO Classification of Tumours: Soft Tissue and Bone Tumours, published in 2020, includes four neoplasms of notochordal differentiation, three malignant [conventional chordoma (CC), dedifferentiated chordoma (DC) and poorly differentiated chordoma (PDC)], and one benign [benign notochordal cell tumor (BNCT)] [1]. BNCT and CC are the more common and established tumors of notochordal differentiation with DC and PDC being newly designated in the WHO classification of bone tumors in 2020 as compared to the previous 2013 edition [1]. CC is a malignancy with a phenotype that recapitulates notochord and primarily affects the axial skeleton [1]. CC was initially thought to be of cartilaginous origin and named "ecchordosis physaliphora" by Virchow in 1857 [2]. This lesion was renamed "chordoma" by Steiner and Ribbert in 1894 [3]. DC represents a biphasic lesion with high grade sarcoma arising in an otherwise CC [1]. PDC is the most recently described of these lesions and is poorly differentiated but maintains notochord differentiation [1]. In contrast to CC, BNCT is a more recently described entity, proposed by Dr. Joseph Mirra at the 1996 International Skeletal Society meeting and published in 2001 and represents a nonaggressive lesion of the axial skeleton and has also been referred to as benign chordoma, benign notochordal cell lesion, giant notochordal rest, giant notochordal hamartoma, and ecchordosis physaliphora vertebralis [4, 5].

Lesion location and the intrinsic radiologic appearance are often highly suggestive of either BNCT or chordoma, allowing distinction from other potential diagnoses. This article reviews and illustrates the clinical characteristics, pathologic features, imaging appearance spectrum, treatment, and prognosis of BNCT and spinal chordoma.

Notochordal hypotheses of origin

The notochordal hypothesis of origin of chordoma and BNCT was initially supported by the animal experiments and human autopsies of Müller [6]. The embryonal notochord is composed of mesodermal cells and provides a semirigid scaffold for the developing vertebral column. As the surrounding sclerotomes form vertebral bodies, the notochordal cells involute except residua in the intervertebral disc nucleus pulposus. The incidence of notochordal remnants in humans was reported at 2% by the Steiner and Ribbert 1894 autopsy series [3]. These notochordal remnants are dormant with only a rare incidence of chordoma. This relationship between notochordal remnants and chordoma as well as BNCT origin is further established by their identical overlap of anatomic distribution. Interestingly, chordoma and BNCT do not originate from the disc space but arise from ectopic rests of notochordal cells in the vertebral body [1–6].

Clinical characteristics of BNCT and spinal chordoma

The overall incidence of BNCT in the series of 100 autopsy specimens by Yamaguchi and colleagues was 19% of cadaveric spine specimens [7]. BNCT was present in 11.5% of the clivi, 5% of cervical spines, 0% of thoracic spines, 2% of lumbar spines, and 12% of sacrococcygeal spines at autopsy evaluation (Fig. 1) [7]. Similar notochordal rests located intradurally in the dorsal clival region, referred to as ecchordosis physaliphora spheno-occipitalis, occur in 0.6–2% of autopsy specimens and 1.7% of MR brain examinations [8]. In contradistinction from CC, BNCTs are typically incidental lesions in patients with other causes of back pain detected on CT or more frequently MR [1, 4, 5, 7, 9–11].

CC is a rare primary osseous neoplasm representing only 1–4% of all primary malignant bone tumors [1, 10, 11]. The age adjusted incidence of CC is 8.4 per 10 million population from Surveillance, Epidemiology, and End Results (SEER) data from 1973 to 2009 in the United States (US) [10]. This represents approximately 300 cases annually in the US and 450 in Europe [10, 11]. The vast majority of CCs are sporadic lesions. Familial CCs are rarely reported with an autosomal dominant inheritance pattern and associated with hereditary duplication of the brachyury gene (transcription factor T gene on chromosome 6 q27), a major regulator of notochord formation [12]. Younger patients with the tuberous sclerosis complex (TSC) can also be affected suggesting that inactivation of the TSC1/TSC2 genes may contribute to pathogenesis of notochordal tumors [13].

CC is historically reported to most commonly affect the sacrococcygeal spine (Figs. 2 and 3) followed by the sphenooccipital area and mobile spine segments (C1 to L5) [1, 14, 15]. In a retrospective analysis of 325 CC patients at Mayo Clinic, approximately 50% were sacrococcygeal in location with 33% in the sphenooccipital (clival) region and 17% in the mobile spine [15]. Most scientific studies have confirmed this predilection for the craniocaudal ends of the axial skeleton, particularly the sacrococcygeal region [16–18]. However, a more recent study from American registries (SEER program of the National Cancer Institute) found a near equal distribution among cranial (32%), spinal (33%), and sacrococcygeal (29%) locations [10].

Primary neoplasms of the spine are rare. In a review of 2750 primary bone tumors collected over 42 years, only 126

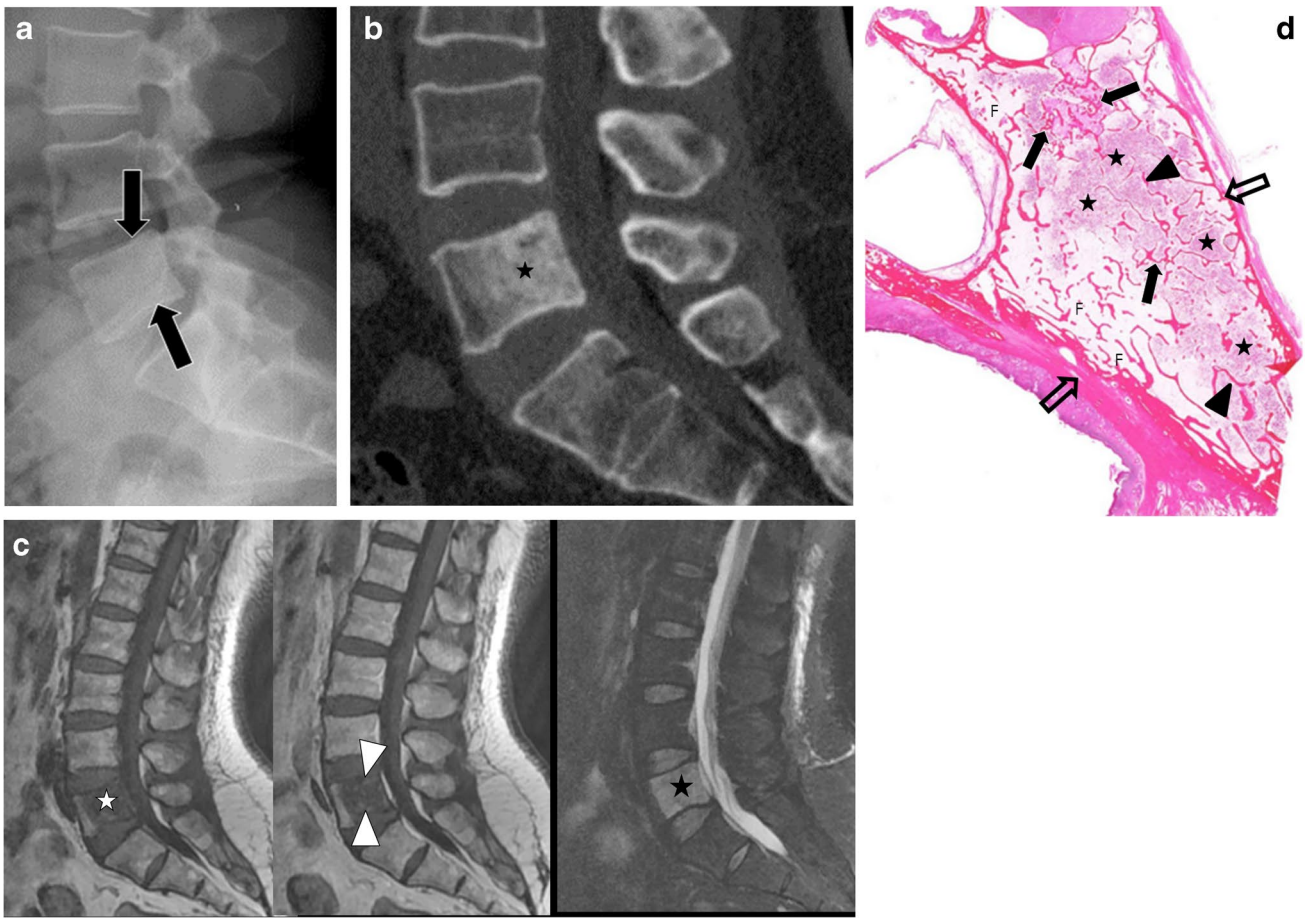

Fig. 1 Benign notochordal cell tumor (BNCT) incidentally discovered in the imaging work-up of low back pain in a 45-year-old man. **a** Lateral radiograph shows mild patchy subtle sclerosis in the posterior L-5 vertebral body (arrows). Bone scan (not shown) was normal. **b** Sagittal CT reveals patchy posterior vertebral body scleroses (black star) but without endplate or posterior vertebral cortex deformity or destruction. **c** Sagittal MR images with T1-weighting (left image in **c** 500/15; repetition time, millisecond/echo time, millisecond), T1-weighting postcontrast (middle image in **c** 600/20) and T2-weighting (right image in **c** 3000/100) with fat saturation demonstrate marrow replacement at L5 (white star) with high signal intensity on T2-weighting (black star) but without contrast enhancement, endplate or cortical destruction, or soft tissue extension. Small areas of higher signal intensity (arrowheads) likely represent regions of maintained yellow marrow typical of BNCT. **d** Photograph of sagittal sectioned whole mount specimen from a different patient with BNCT of the sacrum reveals permeation of the bone marrow by BNCT (black stars) between preexisting trabecula (arrowheads) without their destruction or evidence of lobular growth pattern. Focal thickened trabeculae correspond to areas of sclerosis CT and radiographs (solid arrows). Cortex is intact and not involved (open arrows) without destruction or lesion extension into the soft tissue. Normal yellow marrow containing fat is also apparent (F) beyond the lesion

cases (4.6% of lesions) were spinal in location, including 29 CCs (1.1% of lesions) (of which 23 were sacral) [17]. Sacrococcygeal CCs demonstrate a predilection for the lower sacral segments, particularly the S4-5 segments [1, 16, 18]. CCs of the mobile spine most frequently affect the cervical spine (48% of cases) with a predilection for C2 [18, 19].

CCs affect a wide age range of patients but are most common between 50 and 60 years [1, 10, 16]. The median age at diagnosis is 60 years [1, 10, 16]. A twofold male predilection is reported, and Caucasians are more frequently affected [1, 10, 16]. Spinal CC is typically a slow growing tumor with clinical symptoms often insidious, nonspecific, and location dependent resulting in delayed diagnosis with large lesion size at initial presentation, particularly with sacrococcygeal lesions. Common initial clinical symptoms in sacrococcygeal lesions include back pain, constipation, numbness, gradual onset of neuropathy, and motor weakness. More ominous clinical manifestations related to mass effect such as bowel and/or bladder incontinence, myelopathy, cranial neuropathy, and marked motor weakness are often delayed in sacrococcygeal lesions or associated with mobile spine CCs.

DC is the rarest tumor of notochordal differentiation and can arise de novo or with recurrence of CC [1, 20–22]. DC shows a similar age and location distribution compared to CC with sacrococcygeal region most frequently affected [1,

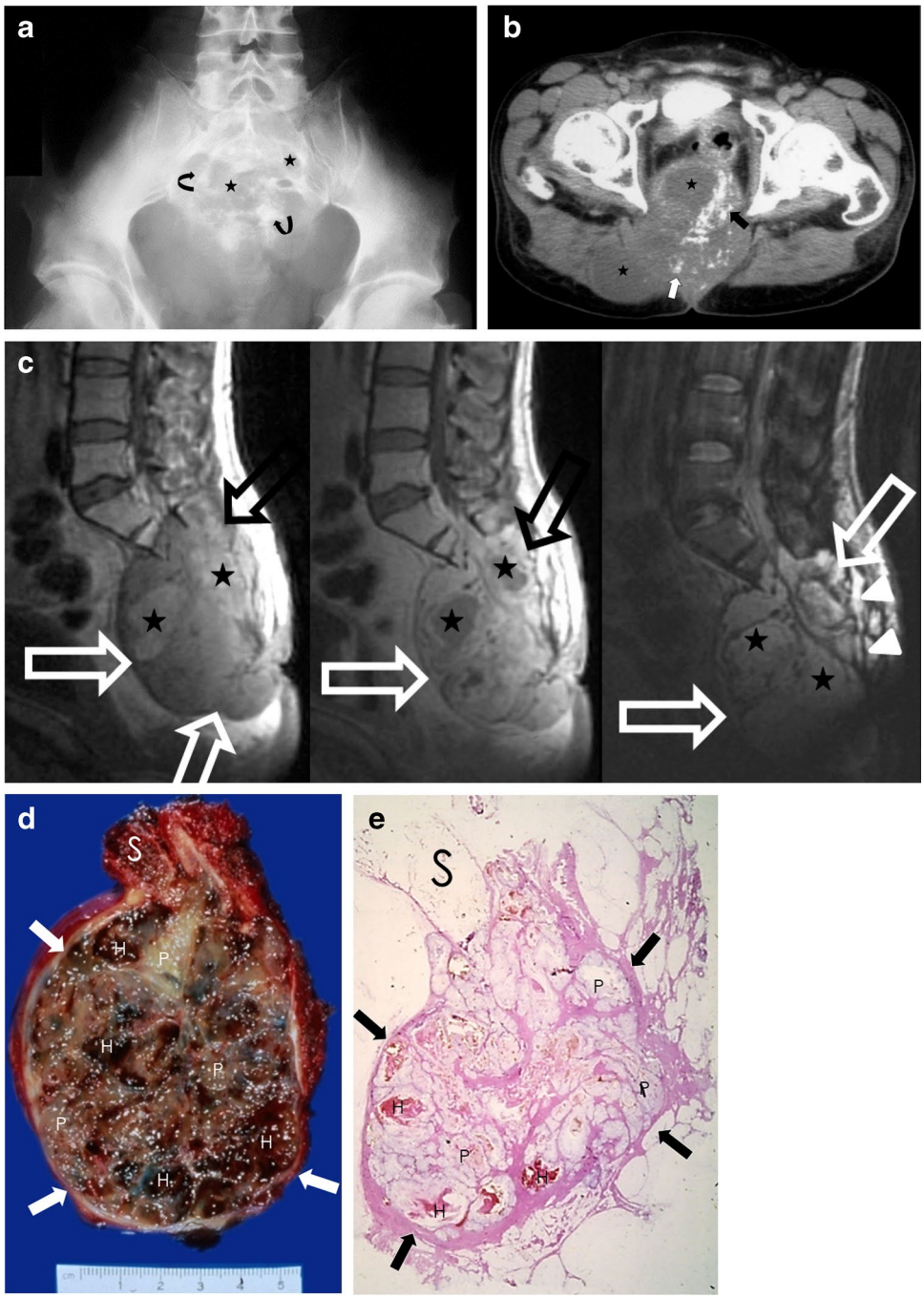

Fig. 2 Sacral chordoma in a 57-year-old man with rectal pain. **a** Frontal radiograph of the pelvis shows a destructive lesion (black stars) with foci of calcification and sclerosis (curved arrows) in the sacrum. **b** Axial CT reveals the large mass replacing the sacrococcygeal spine in the midline with extension into the soft tissues both anteriorly and posteriorly (black stars). Areas of low attention (black stars) and sclerosis and calcification (arrows) are also apparent. **c** Sagittal MR images with T1-weighting (left image in **c** 550/15) and T1-weighting postcontrast (middle image in **c** 500/15) and T2-weighting (right image in **c** 4000/100) demonstrate the large mass replacing the sacrum (open arrows). The mass is multilobulated with areas of hemorrhage [higher signal intensity on T1 and lacking enhancement (**c**, -left and middle images, black stars)] and fluid level posteriorly (**c**, arrowheads). Mild diffuse enhancement is noted on postcontrast MR in nonhemorrhagic regions with high signal intensity on T2 (**c**-right image, black stars). **d**, **e** Photograph of sagittal sectioned gross specimen (**d**) and whole-mount specimen (**e**, hematoxylin and eosin stain) shows the multilobulated mass with replacement of the sacrum and associated anterior and posterior soft tissue components (arrows) and intact upper sacral segment (S). Foci of hemorrhage (H) and high-water content nonhemorrhagic myxoid regions rich in mucopolysaccharides in the physaliphorous areas (P) are seen identically correlating to imaging features

20–22]. Clinical symptoms are also similar to CC, although duration may be shorter and progression more rapid [1, 20–22]. In contradistinction to CC, PDC most commonly affects the clivus or cervical spine and only rarely involves the sacrococcygeal region [1, 22–24]. Patients with PDC are younger than CC with an age range of 1–29 years and a median of 11 years, and there is a female predilection of 2:1 [1, 22–24]. Clinical symptoms are nonspecific with PDC and similar to CC of the mobile spine.

Pathology of BNCT and chordoma

BNCTs are intraosseous lesions composed of sheets or nests of clear cells and a second population of multivacuolated eosinophilic cells (Fig. 4) [1, 4, 5, 9, 25]. The clear cell vacuoles push the nucleus to the side creating an adipocyte-like appearance [1, 4, 5, 9, 25]. The characteristic physaliphorous cells with multiple, clear cytoplasmic vacuoles that indent or entrap the nucleus

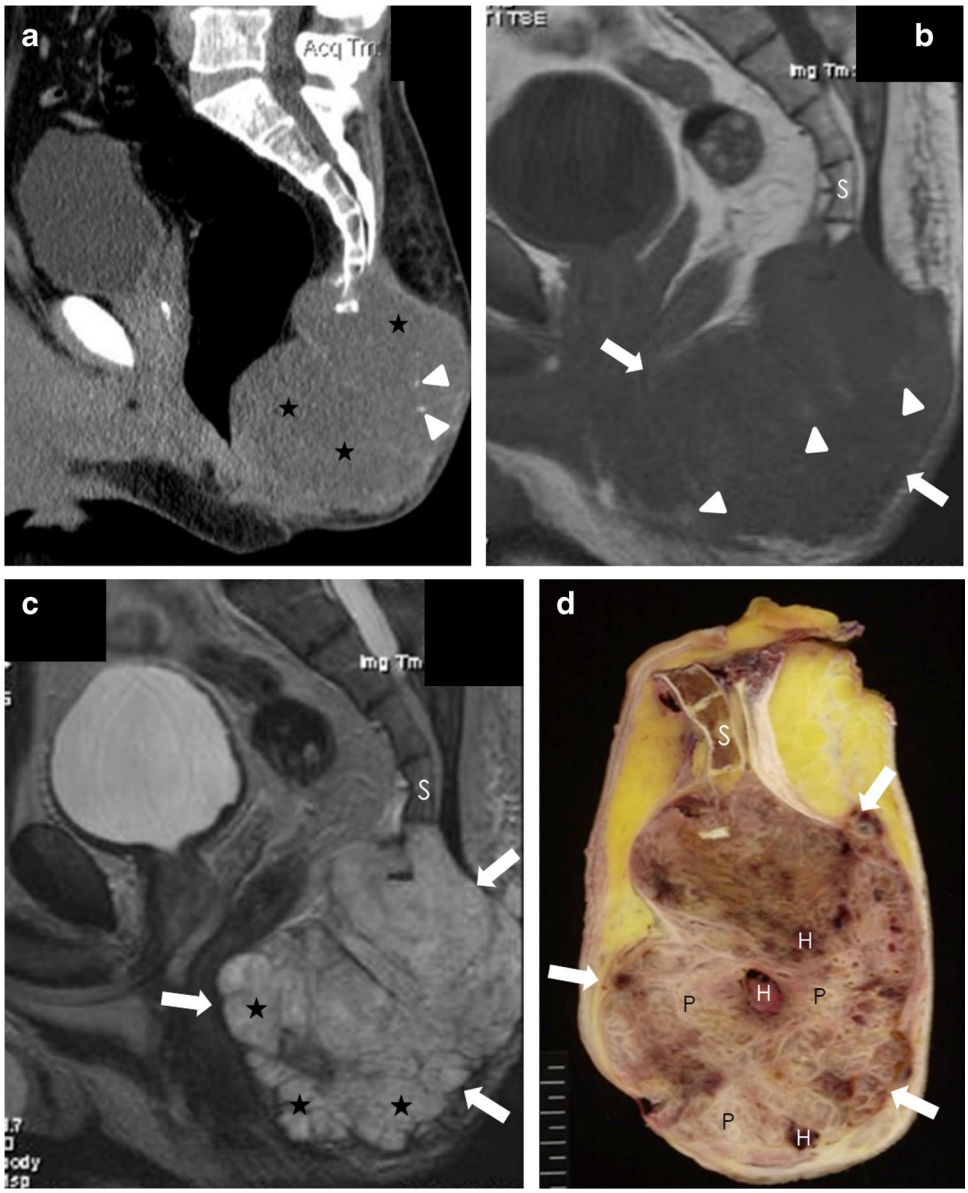

Fig. 3 Chordoma involving the lower sacrum and coccyx in a 60-year-old man with perirectal pain and discomfort. **a** Sagittal CT reveals extensive lower sacral and coccygeal destruction with large associated anterior and posterior soft tissue components with low attenuation (black stars) and small areas of calcification (arrowheads). **b** Sagittal T1-weighted (**b** 400/15) and sagittal T2-weighted (**c** 3000/100) MR images demonstrate the large sacrococcygeal mass with anterior and posterior soft tissue components (arrows). There is low to intermediate signal intensity on T1-weighting (**b**) and multilobulated high signal intensity on T2-weighting) (**c,** black stars). Small subtle areas of high signal intensity on T1-weighting (**b**, arrowheads) represent hemorrhage. The lesion is centered in the midline. Noninvolved upper sacral segments (S) are noted. **d** Photograph of sagittally sectioned gross specimen shows identical characteristics as seen on imaging with the large destructive lesion involving the lower sacrum and coccyx, large multilobulated associated soft tissue mass (arrows) and sparing of the upper sacrum (S). Areas of hemorrhage (H) and high water content nonhemorrhagic myxoid regions (P) are also seen

are admixed in these lesions (Fig. 4). In contradistinction to CC, BNCT permeates between the existing trabecular architecture (which may be thickened owing to reactive appositional bone formation) without causing bone resorption/destruction, are well defined with demarcation from surrounding tissue and lack cortical permeation or associated soft tissue mass (Figs. 1 and 4). In addition, BNCT lacks necrosis, myxoid matrix, cording, mitotic activity, syncytia, or fibrous septa (Fig. 4) [1, 4, 5, 9, 25]. At autopsy, the average size of BNCT is small (approximately 2 by 4 mm), although rarely lesions may involve the entire vertebral body [25]. The term atypical notochordal cell tumor (ANCT) has recently been suggested for lesions that show histologic features of BNCT (other than focal myxoid changes) but may reveal minute areas of soft tissue extension [26]. The ANCTs described by Carter and colleagues revealed only minimal to no progression over 3–10-year follow-up [26].

On gross examination, CCs are large gelatinous, multilobulated, and semitranslucent-to-gray intraosseous tumors and invariably extend into adjacent soft tissues (Figs. 2 and 3) [1, 14, 16]. The associated soft tissue mass typically compresses adjacent tissue, resulting in a pseudoencapsulation [1, 14, 16]. CCs are composed of strands, cords, or syncytia of tumor cells in pale blue pools of myxoid stroma separated by fibrous septa and the characteristic physaliphorous cells (Fig. 4) [1, 14, 16]. The nuclei vary from bland to anaplastic. Mitotic activity is low or not present [1, 14, 16]. Necrosis and hemorrhage (Figs. 2 and 3) are frequent and may be extensive. Lesions may mimic hyaline cartilaginous

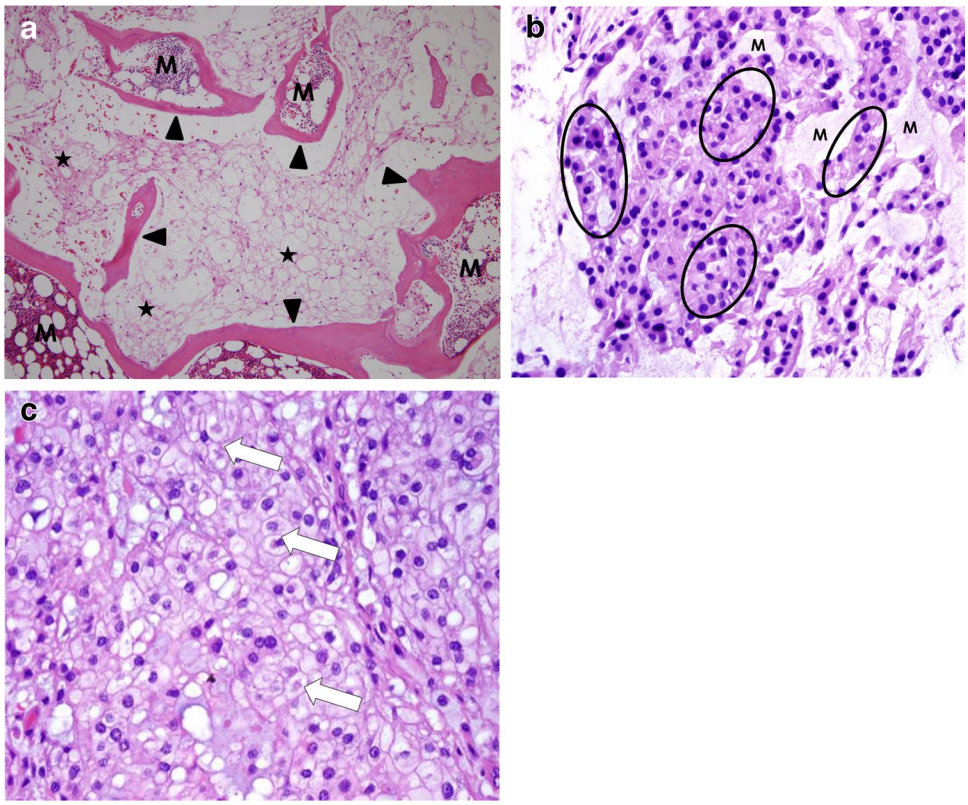

Fig. 4 Histology of both benign notochordal cell tumor (BNCT) and chordoma. **a** High powered photomicrograph of BNCT (original magnification, × 10, hematoxylin–eosin stain) showing notochordal tissue (black stars) infiltrating and permeating, but not destroying, between preexisting trabecular bone (arrowheads) with areas of normal hematopoietic tissue (M). **b**, **c** High power photomicrographs (original magnification, × 40, hematoxylin–eosin stain) reveal typical features of chordoma with epithelioid cells arranged in anastomosing cords and nests (**b**, open ovals) replacing normal marrow with myxoid background (M) and more vacuolated physaliphorous cells (**c**, arrows). Brachyury immunohistochemistry stain (not shown) revealed strong nuclear staining in these cells

neoplasms. The immunohistochemical profile of BNCT and CC is similar and express S-100, EMA, cytokeratins AE1/AE3/CAM5.2, and brachyury [1, 9, 12, 14, 16, 26]. Brachyury is a more recently described regulator of notochordal development that has also proven useful in differentiating chordoma from other histologic mimics including a cartilaginous neoplasm (Fig. 4) [1, 12, 26]. Cytogenetic abnormalities in CC include monosomy of chromosome 1 and gain at chromosome 7 [1, 26–29]. Additionally, homozygous or heterozygous loss of CDKN2A and CDKN2B has been reported in up to 70% of chordomas [1, 26–29].

The relationship between BNCT and CC is controversial. BNCT and CC can coexist. In a series of 46 chordomas, Shen and colleagues identified 7% of CC with coexistent BNCT components and in 13% areas of BNCT that were spatially separate from sacrococcygeal CC [30]. Yamagucchi and coworkers have also suggested malignant transformation of BNCT [31]. We would agree with Carter and colleagues that "currently there is no direct proof of a causal relationship between BNCT and CC" [26].

Two recently described variants of chordoma are DC and PDC. DC represents a biphasic lesion showing areas of CC and a high-grade component typically composed of undifferentiated pleomorphic spindle cell tumor, osteosarcoma, fibrosarcoma, or rarely rhabdomyosarcoma [1, 20–22]. PDC is composed of epithelioid cells often in a cohesive and sheet-like pattern and lacks the typical features of CC such as extracellular matrix and characteristic physaliphorous cells [1, 22–24]. Immunohistochemistry markers similar to CC include cytokeratin and most importantly brachyury positivity but lack S100 and show loss of SMARCB1 (INI1) [1, 22–24].

Imaging of spinal BNCT

BNCTs are most commonly occult at radiography, particularly in the typical small lesion (Fig. 1). Larger BNCTs may reveal mild subtle areas of sclerosis (Fig. 1). Lesions are frequently midline. Similarly, bone scintigraphy and PET imaging are commonly normal in BNCT without significant areas of radionuclide uptake [1, 4, 5, 31, 32]. Mildly reduced radionuclide uptake is also described [1, 4, 5, 31, 32].

BNCTs reveal patchy areas of sclerosis at CT, without regions of associated osteolysis (Fig. 1). Lesions are typically less than 35 mm in size and only rarely involve larger areas of the vertebral body [1, 4, 5, 7, 25, 33–37]. This sclerosis often is seen between a focally maintained trabecular architecture, particularly at the lesion periphery, correlating with the infiltration but lack of trabecular destruction seen histologically (Fig. 1).

On MR, BNCT demonstrates low to intermediate signal intensity on T1-weighted images and high signal intensity with mild heterogeneity on T2-weighting (Fig. 1). These

intrinsic features, similar to CC, reflect the myxoid component (high-water content) histologically [1, 4, 5, 7, 25, 33–37]. Similar to CT, the presence of minute foci of high signal intensity representing maintained normal yellow marrow on T1-weighted MR images has been described and also corresponds to the infiltration of notochordal tissue between trabeculae seen histologically (Fig. 1c) [1, 7, 25]. Following administration of intravenous contrast, most reports demonstrate no or minimal contrast enhancement (Fig. 1c) in BNCT at CT or MR imaging [1, 7, 25, 33–37]. No evidence of cortical destruction, penetration, or associated soft tissue mass is seen in BNCT at CT or MR (Fig. 1).

Imaging of spinal chordoma

The radiographic appearance of sacrococcygeal CC is typically of a large mixed lytic and sclerotic lesion with prominent osseous expansile remodeling and associated presacral soft tissue mass (Figs. 2 and 3) [1, 18, 31, 38]. The regions of sclerosis correspond to small punctate areas of amorphous calcification, seen in 50–70% of cases radiographically (Fig. 2) [1, 18, 31, 38].

CC of the mobile spine is invariably centered in the vertebral body (Fig. 5). These lesions less commonly demonstrate punctate areas of calcification compared to sacrococcygeal lesions, seen in only approximately 30% of cases radiographically (Fig. 5) [1, 18, 31, 38]. However, areas of vertebral sclerosis are frequent (43–62% of cases) unlike sacrococcygeal lesions [1, 18, 31, 38]. Vertebral body sclerosis is infrequently the dominant feature on radiographs leading to an "ivory vertebral body" appearance (Fig. 5). Bone destruction is more commonly the predominant feature radiographically and may be associated with pathologic fractures. CC of the mobile spine may also involve the adjacent vertebral bodies in 11–14% of cases [18, 31, 38–43]. Small CC may be occult radiographically, particularly in the anatomically complex sacrococcygeal and mobile spine regions in approximately 5–10% of cases [42, 43].

There are only limited nuclear medicine studies of chordomas reported in the literature. Bone scintigraphy typically reveals increased heterogeneous uptake of radionuclide of varying degree from mild to marked in greater than 90% of cases [32, 41–47]. Photopenia can also occur, although unusual in our experience, and is more likely in small lesions. Gallium scans and 68 GA-DOTA-TATE also reveal increased radiotracer uptake in spinal chordoma [44]. 18-fluorodeoxyglucose positron emission tomography (FDG-PET) also shows moderate heterogeneous increased radionuclide activity and high standardized update values (SUV, average maximum of 5.8) in spinal chordomas [32, 44, 47]. FDG-PET including C-methionine-PET may be useful for therapeutic monitoring in chordoma, as with other nonmusculoskeletal malignancies [45].

CT of sacrococcygeal CC typically reveals a predominantly lytic lesion (Figs. 2 and 3). Associated soft tissue masses, more prominent anteriorly, are invariably present (Figs. 2 and 3). Lesion margins are often lobular reflecting the pathologic growth pattern and are commonly well-defined owing to pseudocapsule formation (Figs. 2 and 3). Multiple punctate areas of calcification are frequently seen in 60–90% of cases, more often located centrally (Figs. 2 and 3) [39–42, 46, 47]. Areas without calcification are usually lower attenuation compared to skeletal muscle reflecting the myxoid component of these lesions (Figs. 2 and 3) [39–42, 46, 47]. Postcontrast CT commonly shows a mild and diffuse or peripheral/septal degree and pattern of enhancement [39–42]. Mobile spine CC demonstrates similar CT features with additional vertebral body sclerosis (Fig. 5). Anterior paraspinal components are typically larger than anterior epidural extensions.

MR of sacrococcygeal CC frequently reveals a large area of marrow replacement with an associated soft tissue mass (Figs. 2 and 3) [43, 46, 47]. The associated soft tissue mass is larger in the presacral region (Figs. 2 and 3) and was present in 100% of the 30 cases described by Sung and coworkers [46]. Presacral soft tissue components alone are present in 23% of cases [46]. However, posterior soft tissue components (77% of cases) are also frequent [46]. Lesion margin may be well-defined (70–100%) or ill-defined (0–30%) and a lobular growth pattern (70%) is frequent with associated septations (100%) [43, 46]. The signal intensity on T1-weighted and T2-weighted MR is predominantly low to intermediate (83–100%) and high signal (92–100%), respectively, reflecting these lesions high myxoid content (Figs. 2 and 3) [43, 46, 47]. Areas of high signal intensity on both T1-weighted and T2-weighted MR, representing hemorrhage (Figs. 2 and 3), are common and seen in 66–77% of cases [43, 46, 47]. Low signal intensity foci on all MR pulse sequences are also common, likely representing calcification and hemosiderin. This combination of components causes heterogeneity on all MR sequences. While joint involvement by neoplasm is unusual in most locations, 23% of cases of sacrococcygeal CC revealed SI joint transgression in one study [46]. In our experience, this is more frequent in upper sacral CC with extension into the ligamentous portion of the SI joint which lacks protective cartilage [48, 49].

The MR enhancement pattern of sacrococcygeal chordoma following intravenous contrast administration is variable in degree and pattern (Fig. 2). The degree of enhancement is typically mild to moderate (65–80%) with marked enhancement seen in only 20–35% of cases [39, 41, 43, 46, 47]. The most common patterns of enhancement may be heterogeneous (95%) and diffuse or peripheral/septal with areas of nodularity [43, 46, 47].

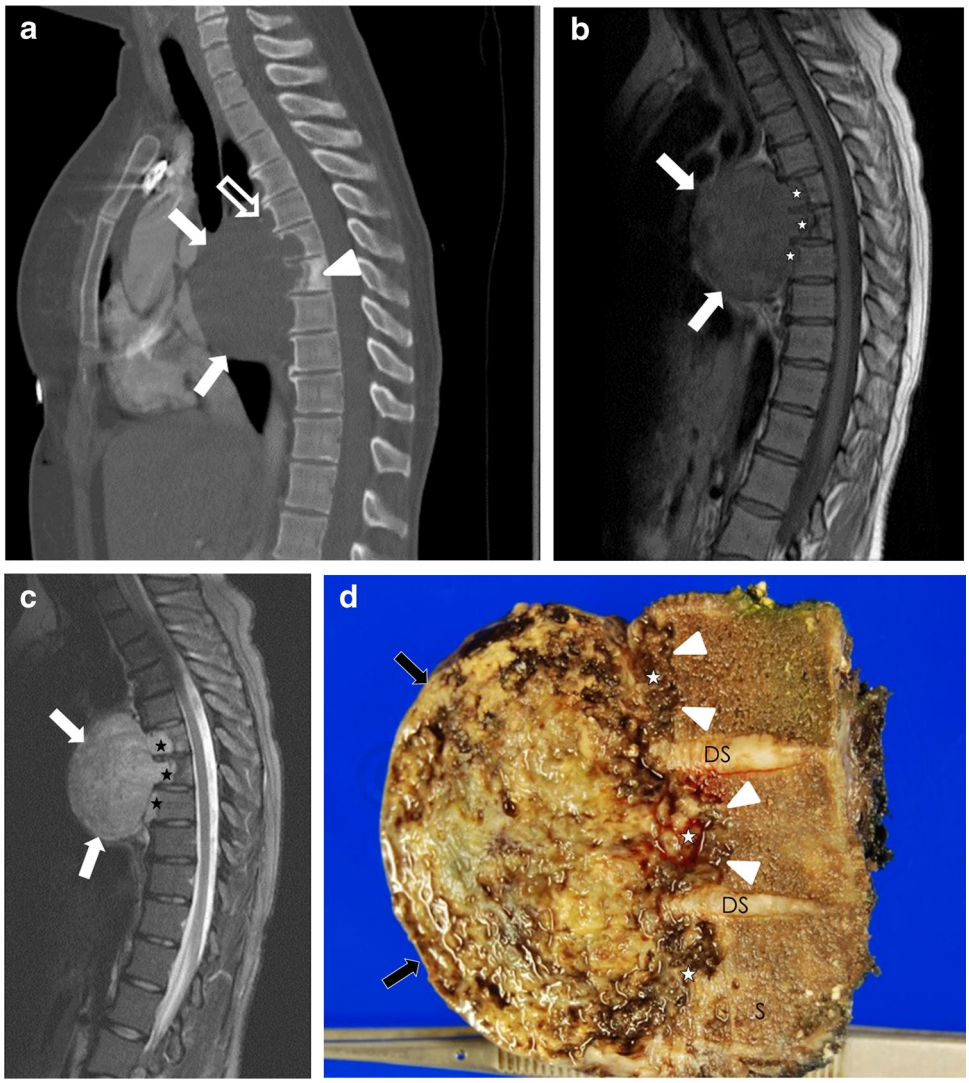

Fig. 5 Spinal chordoma of the thoracic region in a 65-year-old man with pain and radicular symptoms. **a** Sagittal CT image shows a multilevel vertebral lesion centered at T7 with a large associated anterior soft tissue mass (solid arrows) which has decreased attenuation reflecting high water content and small focus of calcification (a-open arrow). There is more diffuse sclerosis of T7 (arrowhead) creating an "ivory" vertebral body. **b**, **c** Sagittal MR images with T1-weighting (**b** 500/15) and T2-weighting (**c** 4000/120) reveal multilevel vertebral body involvement (black and white stars) with large associated anterior tissue mass (arrows). The anterior soft tissue mass shows intermediate signal intensity on T1-weighting (**b**, arrows) and high signal intensity on T2-weighting (**c**, arrows). The lesion extends around the maintained disc spaces to involve multiple spinal levels (black and white stars) as opposed to extending through the disc spaces. **d** Photograph of sagittal sectioned gross specimen demonstrates the multilevel spine involvement (white stars) with more diffuse infiltration of T7 including posterior sclerosis (S) and large associated soft tissue mass (arrows). The involvement of additional levels is seen extending around but not through the disc spaces (DS) with invasion of the vertebral bodies anteriorly (arrowheads) identical to the features seen on imaging

Mobile spine CC has similar intrinsic MR features described for sacrococcygeal lesions (Fig. 5). The marrow replacement on T1-weighting may create a "pseudobrain" MR imaging appearance which has been described as pathognomonic for plasmacytoma [50]. The anterior paraspinal and anterior epidural soft tissue components are optimal evaluated by sagittal MR (Fig. 5).

Multilevel involvement by CC of the mobile spinal segments may simulate infectious spondylodiscitis. However, in our experience, these lesions more commonly extend around the disc to affect adjacent spinal segments, sparing the disc space, as opposed to transdiscal extension. This disc space sparing is optimally depicted on cross-sectional imaging, particularly MR (Fig. 5). These imaging features of a large associated soft tissue mass, disc space sparing, and lack of prominent surrounding soft tissue edema allow accurate distinction from infectious spondylodiscitis.

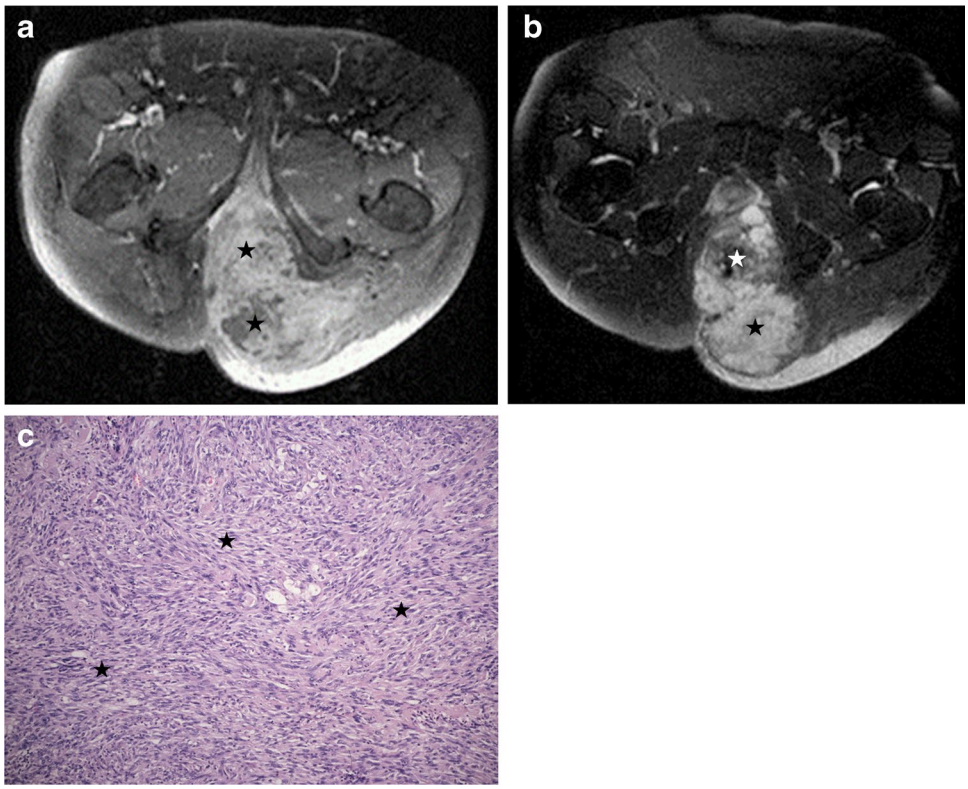

Fig. 6 Sacral chordoma with dedifferentiation in a 67-year-old woman with sacral pain and palpable mass. **a**, **b** Axial MR images including T1-weighting postcontrast fat suppresed (**a**, 520/15) and T2-weighting with fat suppression (**b**, 3000/60) reveal sacrococcygeal destruction with anterior and posterior soft tissue components (black and white stars). The anterior soft tissue component has more enhancement (**a**) and has lower signal intensity on T2-weighting (**b**) and represents dedifferentiation. **c** High-power photomicrograph (original magnification × 20, hematoxylin–eosin stain) of the dedifferentiated areas reveals typical fascicular and storiform pattern of spindled cells (black stars) representing a region of undifferentiated pleomorphic sarcoma. Other regions (not shown) demonstrated typical chordoma histology with positive brachyury immunohistochemistry staining

Local recurrence of CC typical reveals a new soft tissue mass in the postoperative site on cross-sectional imaging with similar intrinsic characteristics of the original lesion [51, 52].

Cross-sectional imaging of DC or PDC may show differences compared to CC reflecting more cellular tissue containing less myxoid components (Figs. 6 and 7) [1, 20–24]. On CT, these areas may reveal higher attenuation, similar to muscle. On MR, these histologic variants of chordoma may demonstrate intermediate signal intensity on both T1-weighted and on long TR MR sequences (Figs. 6 and 7) [1, 20–24]. Focal areas (DC) or more diffuse regions (PDC) of prominent enhancement may also be seen (Fig. 6) [1, 21–24]. Diffusion-weighted MR may also reveal lower ADC values in these lesions compared to CC reflecting this higher degree of cellularity [1, 20–24, 53].

Differentiating imaging features of BNCT and CC

The most significant discriminators favoring the diagnosis of BNCT in contradistinction to chordoma are sclerosis with maintenance of the trabecular architecture, no component of osseous or cortical bone destruction, absence of an associated extraosseous component, and the lack of contrast enhancement on MR (Fig. 8) [1, 4, 7, 9, 25, 26, 29–31, 33–37]. Atypical imaging features of BNCT include evidence of significant contrast enhancement, minimal interval growth (1–2 mm per year), foci of bone lysis, and minute soft tissue components (Fig. 8) [26, 54]. We would agree with Carter and coworkers and advocate the use of the term ANCT for lesions with unusual imaging features of typical BNCT (Fig. 9) [26, 54]. ANCT requires close clinical and imaging follow-up to limit overly aggressive treatment, when balanced with the risk of neurologic complications, and surgical resection may not be warranted in the appropriate clinical scenario [26, 54]. In contradistinction, a notochordal neoplasm with significant cortical destruction and associated soft tissue component is a definitive CC and requires aggressive treatment (Figs. 2, 3, 5, and 8).

Treatment of spinal BNCT and chordoma

Biopsy of incidentally discovered BNCT, on CT or more likely MR with typical imaging features, is usually not warranted (Figs. 1 and 8). In fact, biopsy of BNCT may provoke misdiagnosis for CC, leading to extensive surgical resection and unintended postoperative complications [26, 54]. Long-term imaging follow-up of BNCT may be considered with CT and/or MRI to ensure no significant interval change occurs [26, 54].

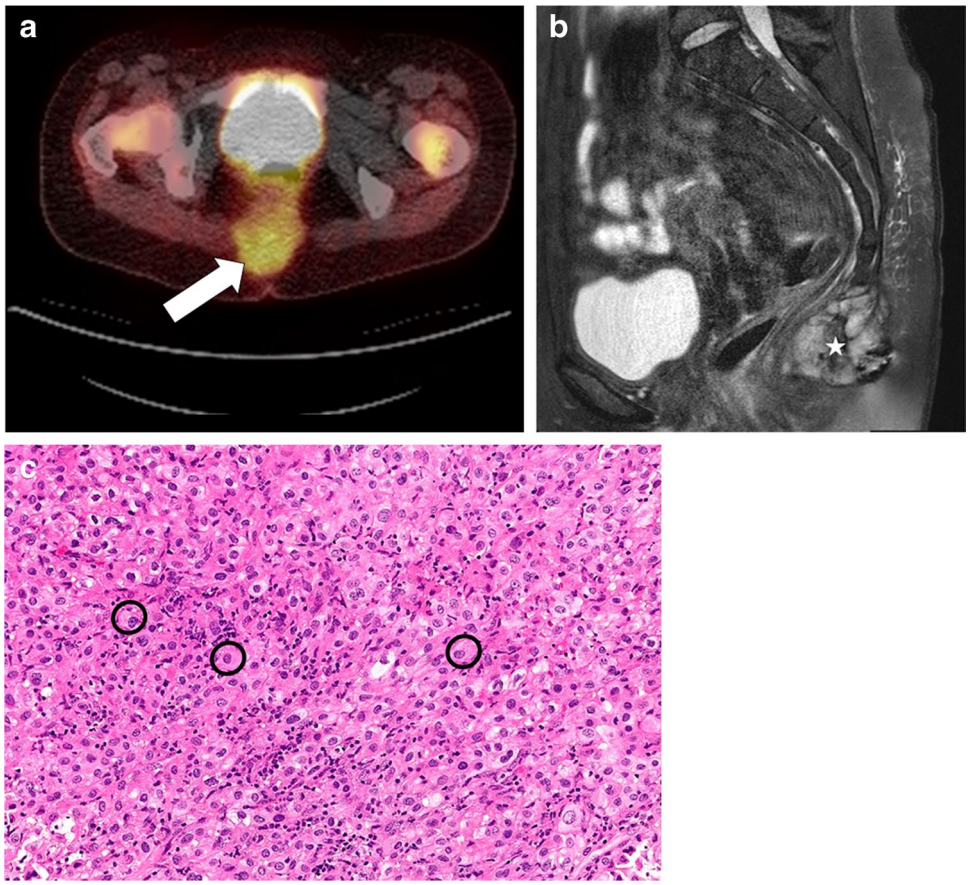

Fig. 7 Poorly differentiated chordoma of the sacrococcygeal region in a 34-year-old woman with 6 years of sacral pain initially recognized after child birth. **a** Axial PET-CT shows midline destructive sacrococcygeal mass (arrow) with prominent radionuclide uptake. **b** Sagittal T2 weighted fat suppressed (**c**, 4000/60) MR image reveals the sacrococcygeal midline destructive lesion with soft tissue extension. There is lower signal intensity on T2-weighting (**b**, white star) than often seen in typical chordoma. **c** High power photomicrograph (original magnification, ×40; hematoxylin–eosin stain) demonstrates sheets of mitotically active epithelioid cells with oval and irregular nuclei and eosinophilic cytoplasm without typical features of chordoma (open circles). There are intermixed small inflammatory cells. However, on immunohistochemistry stains (not shown), there was nuclear positivity for brachyury and nuclear INI-1 loss representing poorly differentiated chordoma (case courtesy of Drs. Miriam A. Bredella and Yin P. Hung)

Despite its reported low-grade biologic behavior with slow growth, CC presents numerous treatment challenges for effective control. The tumor is often large at presentation and adjacent to critical normal structures that impede complete resection and hinder effective radiation therapy [55–69]. Management of these complex cases is best accomplished at large multidisciplinary centers that possess sufficient experience to facilitate maximal function and minimize side effects [55–67].

Since the 1970s, a wide en-bloc resection is the cornerstone of surgical resection of sacrococcygeal CC (Figs. 2 and 3) [55–67]. Achieving a wide surgical margin is the most important predictor of survival and local recurrence [55–67]. Surgical excision necessitates resection of at least one entire sacral segment beyond the area of gross disease [56]. Numerous studies have documented the hazard of transgressing the tumor margin with nearly twice the recurrence rate associated with pseudocapsule violation [55–67]. Similarly, subtotal resection of these tumors predisposes to increased local recurrence rates [55–67].

The surgical approach is dictated by the extent of the tumor [56, 65, 67, 68]. Resection of tumors inferior to the SI joint (caudal to S3) typically involves a posterior-transperineal exposure. On the other hand, chordoma arising above the inferior portion of the SI joint (cephalad to S3) necessitate a combined anterior–posterior approach [56, 65, 67, 68]. Low sacral amputation involves the sacrifice of at least one S4 nerve root and below [56, 65, 67, 68]. Mid-sacral amputation involves the removal of at least one S3 nerve root and below [56, 65, 67, 68]. High sacral amputation involves the sacrifice of at least one S2 nerve root and below [56, 65, 67, 68]. Total sacrectomy involves resection above the S1 level [55–68].

Achieving a wide margin is the primary surgical goal of chordoma resection, but unfortunately also often

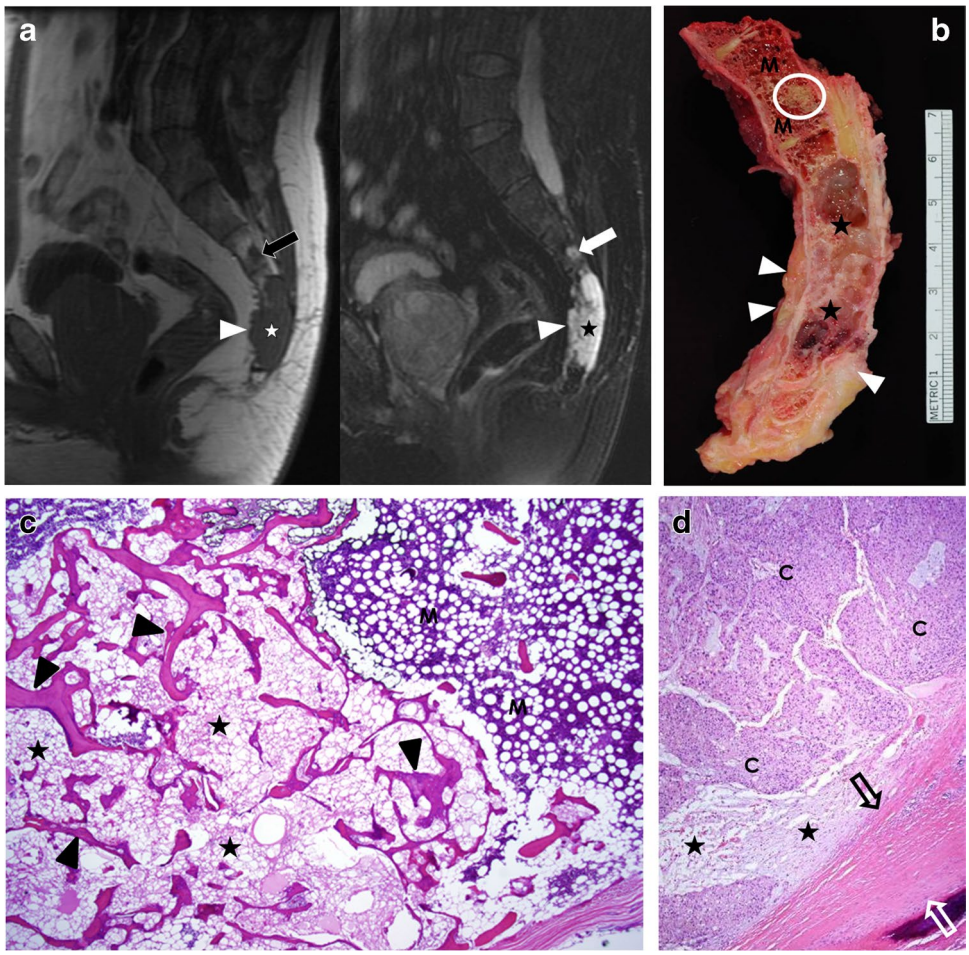

Fig. 8 Sacral chordoma and coexistent benign notochordal cell (BNCT) tumors in a 64-year-old man with sacrococcygeal pain worsened with sitting. **a** Sagittal T1-weighted (left image, **a** 500/15) and fat suppressed T2-weighted (right image, **a** 4000/100) MR images show marrow replacement in the lower sacrum on T1-weighting (left image, **a** white star) with high signal intensity on T2-weighting (right image, **a** black star). There is anterior soft tissue extension (arrowheads) representing chordoma. A second small foci with similar intrinsic signal characteristics is seen at S3 (arrows) without soft tissue extension representing a BNCT. **b** Photograph of sagittal sectioned gross specimen reveals the lower sacral chordoma (black stars) with both anterior and posterior soft tissue extension (arrowheads). BNCT at S3 (open circle) demonstrates normal surrounding marrow (M) and lacks soft tissue extension. **c** Medium power photomicrograph (original magnification, × 10; hematoxylin–eosin stain) shows infiltration and permeation of the BNCT (black stars) between thickened trabeculae (arrowheads) without destruction and adjacent normal marrow (M). **d** Medium power photomicrograph (original magnification, × 10; hematoxylin–eosin stain) reveals chordoma with myxoid region (black stars) and other cellular areas of sheets and cords of epithelioid cells (C) replacing and destroying the marrow with extension into the soft tissue and fibrous pseudocapsule formation (between open arrows)

sacrifices functionally important nervous and osseous structures [56, 65, 67, 68]. When possible, preservation of the S2 nerve root during the sacrectomy is highly desirable to prevent loss of voluntary bowel/bladder control [56, 65, 67, 68]. Sparing of the S2 nerve roots bilaterally is associated with up to a 50% chance of normal bladder/bowel function and an even higher likelihood if at least one S3 nerve root is also preserved [56, 65, 67, 68]. Complete spinal-pelvic dissociation and total sacrectomy with sacrifice of the S1 nerve roots causes marked ambulation difficulties and neurologic damage and requires internal fixation for mechanical stabilization [56, 65, 67, 68].

For mobile spine chordomas, advancements in surgical techniques involving spondylectomy, corpectomy and instrumented cage devices have permitted increased use of en-bloc resection (Fig. 5) [55, 57, 60, 61, 70, 71]. As with other chordomas, there are inherent challenges primarily related to the presence of nerve roots, paraspinal/vertebral arteries, and complex osseous anatomy with increased risk of neurologic deficits and local recurrence [55, 57, 60, 61, 70, 71].

Conventional radiation therapy is largely ineffective for treatment or control of CC in the absence of total surgical resection [38, 64, 68, 69, 72]. The proximity of the

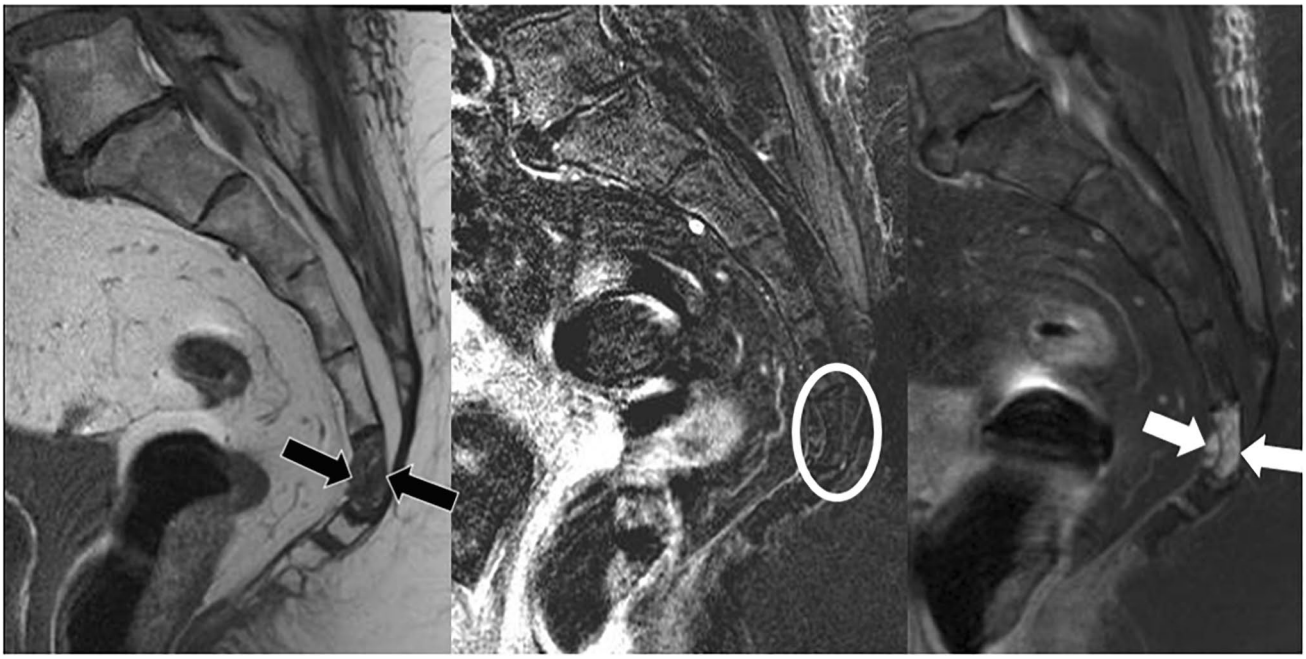

Fig. 9 Atypical notochordal cell tumor (ANCT) incidentally discovered on MR imaging of the pelvis in a 60-year-old female. Sagittal MR images with T1-weighting (left image, 500/20), T1-weighting postcontrast fat suppressed subtraction (middle image, 600/20) and fat suppressed T2-weighting (right image, 3500/20) show a marrow replacing lesion at S5. The lesion reveals low/intermediate signal intensity on T1-weighting (left image, black arrows), no enhancement (middle image, open circle), and high signal intensity on T2-weighting with fat suppression (right image, white arrows). There is a minute anterior soft tissue component. Lesion was biopsied and confirmed as ANCT (case courtesy of Dr. Mark J. Kransdorf)

spinal cord, spinal/cranial nerves, and rectum precludes the administration of higher photon radiation therapy doses (45–80 Gy) in many cases [38, 64, 68, 69, 72]. Lower doses (40–60 Gy) are associated with significantly poorer local control (only 10–40% at 5 years) [38, 64, 68, 69, 72]. Early studies using proton beam or charged particle radiotherapy have shown superior rates of local control (50–60% at 5 years for chordomas involving the skull base, cervical spine, and sacrococcygeal region) [38, 64, 68, 69, 72]. The combination of proton-beam radiotherapy and wide en-bloc resection is now often the preferred treatment protocol [38, 64, 68, 69, 72]. As proton therapy delivers less radiation to surrounding tissues compared to conventional radiotherapy, a higher dose can reach the target tissue leading to greater desired effects [38, 64, 68, 69, 72].

Local recurrence of chordoma is common despite optimal initial therapy [38, 68, 71–74]. Local recurrence is directly related to the ability to accomplish complete initial surgical resection which is only successful in 35–75% of sacrococcygeal CC (Figs. 2 and 3) and 21% of mobile spine lesions (Fig. 5) [38, 68, 71–74]. Reexcision and reirradiation are typically employed, although toxicities from prior radiation effects and technical challenges affiliated with additional surgical resection often limit their effectiveness [38, 64, 68–74].

Except for dedifferentiated and poorly differentiated chordoma (Figs. 6 and 7), most chordomas do not respond to conventional systemic chemotherapy [1, 20–24, 38, 68, 72–74]. More novel chemotherapy using molecular-targeting agents such as those focused on platelet-derived growth factor receptors and tyrosine kinase inhibitors has shown promise in early trials [38, 68, 72–74]. Ongoing investigations using therapy targeting epidermal growth factor receptors and transcription factors may also play a role in inhibiting growth and cellular proliferation of these rare tumors [38, 64, 68–74]. The discovery of brachyury resulting from a gene duplication that modulates the development of chordoma has fueled intense speculation and may serve as a focal point for future therapeutic management [38, 64, 68–74].

Prognosis of spinal chordoma

Despite their low-grade biologic behavior, the overall prognosis for CC is guarded at best with most series reporting 5-year survival rates at 45–86%, 10-year survival rates at 28–71% and 20-year survival rates as low as 13% including SEER data from 1973 to 2015 [1, 10, 38, 68]. Several factors are associated with poorer prognosis in the setting of sacrococcygeal CC. Tumors extending more cephalad (above the

S2 or S3 vertebral levels) are reported to have increased rates of local recurrence and decreased survival [1, 10, 38, 68]. In general, larger masses with infiltration of surrounding tissues reveal similar trends, although there is lack of agreement as to what constitutes the critical size [1, 10, 38, 68]. Known technical challenges in achieving en-bloc resection, avoiding intraoperative contamination and possible increased risk of micrometastases in larger tumors contribute to this observation [1, 10, 38, 68]. Local recurrence rates of spine CC have ranged from 19–75% and are significantly more frequent owing to incomplete initial surgical resection [1, 10, 68, 72]. Local recurrence also significantly affects prognosis with a greater than 50% reduction in median survival [1, 10, 58, 68]. Metastatic disease occurs in 3–48% of patients with CC and most frequently affects the lung (54%), bone (20%), soft tissue (15%), and liver (8%) [1, 10, 38, 68, 75]. DC and PDC manifests a more aggressive malignant clinical course with higher rates of local recurrence, metastases, and earlier mortality compared to CC and are associated with a dismal prognosis (Figs. 6 and 7) [1, 20–24, 68].

Summary

Neoplasms of notochordal differentiation include one benign (BNCT) and three malignant (CC, DC and PDC) lesions. These lesions typically involve the spine in an identical anatomic distribution to notochordal remnants with the sacrococcygeal region most frequently affected. This review discusses the imaging appearance spectrum and underlying pathologic basis of BNCT and chordoma. These radiologic features allow detection, characterization, and often differentiation of these lesions.

Acknowledgements The authors gratefully acknowledge the support of Tracee Lee Marshall, Evan B. Greenfield, and former fellows Andrew J. Degnan, MD, and Augustus Suhardja, MD, for manuscript preparation, and without whom this project would not have been possible. We also thank all attendees of the AIRP radiologic pathology courses (past, present, and future) for their contribution to our series of cases.

References

1. Lokuhetty D, White VA, Cree IA, editors. Soft tissue and bone tumours WHO classification of tumours. 5th Ed. France: IARC; 2020. p. 449–457.
2. Virchow RL. Untersuchungen uber die Entwicklung des Shaedelgrundes. Berlin: G Rimer; 1857. p. 566.
3. Steiner H, Ribbert H. Uber die Ecchondrosis physalifora sphenooccipitalis. Centralbl F Path Anat. 1894;5:457–61.
4. Mirra JM, Brien EW. Giant notochordal hamartoma of intraosseous origin: a newly reported benign entity to be distinguished from chordoma: report of two cases. Skelet Radiol. 2001;30(12):698–709.
5. Kyriakos M. Benign notochordal lesions of the axial skeleton: a review and current appraisal. Skelet Radiol. 2011;40(9):1141–52.
6. Müller H. Ueber das Vorkommen von Resten der Chorda dorsalisbeiMenschennachderGeburtund uber ihrVerh altniss zu den Gallertgeschw ulsten am Clivis. Zeitung Fur Rationelle Medzin. 1858;2:202.
7. Yamaguchi T, Suzuki S, Ishiiwa H, Ueda Y. Intraosseous benign notochordal cell tumours: overlooked precursors of classic chordomas? Histopathol. 2004;44(6):597–602.
8. Mehnert F, Beschorner R, Küker W, Hahn U, Nägele T. Retroclival ecchordosis physaliphora: MR imaging and review of the literature. AJNR Am J Neuroradiol. 2004;25(10):1851–5.
9. Tirabosco R, O'Donnell P, Flanagan AM. Notochordal tumors. Surg Pathol. 2021;14(4):619–43.
10. Smoll NR, Gautschi OP, Radovanovic I, Schaller K, Weber DC. Incidence and relative survival of chordomas: the standardized mortality ratio and the impact of chordomas on a population. Cancer. 2013;119(11):2029–37.
11. Pennington Z, Schilling A, Schwab JH, Sciubba DM. In: Sciubba DM, Schwab JH, editors. Chordoma of the spine. Switzerland: Springer; 2021. p. 33–54.
12. Nibu Y, José-Edwards DS, Di Gregorio A. From notochord formation to hereditary chordoma: the many roles of Brachyury. BioMed Res Intern. [cited 2022 Mar 7]2013; 14 p. Available from: https://www.hindawi.com/journals/bmri/2013/826435/. https://doi.org/10.1155/2013/8264355.
13. McMaster ML, Goldstein AM, Parry DM. Clinical features distinguish childhood chordoma associated with tuberous sclerosis complex (TSC) from chordoma in the general paediatric population. J Med Genet. 2011;48(7):444–9.
14. Dahlin DC, Unni KK. Bone tumors: general aspects and data on 8,547 cases. 4th Ed. United States: Charles C. Thomas Pub; 1986. 522 p.
15. Mabrey RE. Chordoma: a study of 150 cases. Am J Cancer. 1935;25(3):501–17.
16. Eriksson B, Gunterberg B, Kindblom LG. Chordoma: a clinicopathologic and prognostic study of a Swedish national series. Acta Orthop Scand. 1981;52(1):49–58.
17. Kelley SP, Ashford RU, Rao AS, Dickson RA. Primary bone tumours of the spine: a 42-year survey from the Leeds Regional Bone Tumour Registry. Euro Spine J. 2007;16(3):405–9.
18. Murphey MD, Andrews CL, Flemming DJ, Temple HT, Smith WS, Smirniotopoulos JG. From the archives of the AFIP. Primary tumors of the spine: radiologic pathologic correlation. Radiographics. 1996;16(5):1131–1158.
19. Bjornsson J, Wold LE, Ebersold MJ, Laws ER. Chordoma of the mobile spine. A clinicopathologic analysis of 40 patients. Cancer. 1993;71(3):735–740.
20. Hung YP, Diaz-Perez JA, Cote GM, Wejde J, Schwab JH, Nardi V, Chebib IA, Deshpande V, Selig MK, Bredella MA, Rosenberg AE, Nielsen GP. Dedifferentiated chordoma: clinicopathologic and molecular characteristics with integrative analysis. Am J Surg Pathol. 2020;44(9):1213–23.
21. Hanna SA, Tirabosco R, Amin A, Pollock RC, Skinner JA, Cannon SR, Saifuddin A, Briggs TWR. Dedifferentiated chordoma: a report of four cases arising "de novo". British JBJS 2008 90-B:5, 652–656.
22. Liu FS, Zheng BW, Zhang TL, Li J, Lv GH, Yan YG, Huang W, Zou MX. Clinicopathologic and prognostic characteristics in dedifferentiated/poorly differentiated chordomas: a pooled analysis of individual patient data from 58 studies and comparison with conventional chordomas. Front Oncol. 2021;V(11).
23. Shih AR, Cote GM, Chebib I, Choy E, DeLaney T, Deshpande V, Hornicek FJ, Miao R, Schwab JH, Nielsen GP, Chen YL. Clinicopathologic characteristics of poorly differentiated chordoma. Mod Pathol. 2018;31(8):1237–45.

24. Yeter HG, Kosemehmetoglu K, Soylemezoglu F. Poorly differentiated chordoma: review of 53 cases. APMIS. 2019;127(9):607–15.
25. Yamaguchi T, Iwata J, Sugihara S, McCarthy EF, Karita M, Murakami H, et al. Distinguishing benign notochordal cell tumors from vertebral chordoma. Skelet Radiol. 2008;37(4):291–9.
26. Carter JM, Wenger DE, Rose PS, Inwards CY. Atypical notochordal cell tumors. Am J Surg Pathol. 2017;41(1):39–48.
27. Vujovic S, Henderson S, Presneau N, Odell E, Jacques TS, Tirabosco R, et al. Brachyury, a crucial regulator of notochordal development, is a novel biomarker for chordomas. Brachyury, a crucial regulator of notochordal development, is a novel biomarker for chordomas. J Pathol. 2006[cited 2022 Mar 7];209(2):157–165. Available from https://www.ncbi.nlm.nih.gov/pubmed/16538613/. https://doi.org/10.2214/ajr.175.1.1750261.
28. Grabellus F, Konik MJ, Worm K, Sheu SY, van de Nes JA, Bauer S, et al. MET overexpressing chordomas frequently exhibit polysomy of chromosome 7 but no MET activation through sarcoma-specific gene fusions. Tumour Biol. 2010;31(3):157–63.
29. Ulici V, Hart J. Chordoma: a review and differential diagnosis. Arch Pathol Lab Med. 2022;146(3):386–95.
30. Shen J, Li CD, Yang HL, Lu J, Zou TM, Wang DL, et al. Classic chordoma coexisting with benign notochordal cell rest demonstrating different immunohistological expression patterns of brachyury and galectin-3. J Clinl Neurosci. 2011;18(1):96–9.
31. Yamaguchi T, Yamato M, Saotome K. First histologically confirmed case of a classic chordoma arising in a precursor benign notochordal lesion: differential diagnosis of benign and malignant notochordal lesions. Skelet Radiol. 2002;31(7):413–8.
32. Park SA, Kim HS. F-18 FDG PET/CT evaluation of sacrococcygeal chordoma. Clin Nucl Med. 2008;33(12):906–8.
33. Nishiguchi T, Mochizuki K, Ohsawa M, Inoue T, Kageyama K, Suzuki A, et al. Differentiating benign notochordal cell tumors from chordomas: radiographic features on MRI, CT, and tomography. AJR Am J Roentgenol. 2011;196(3):644–50.
34. Chauvel A, Taillat F, Gille O, Rivel J, Vital JM, Bioulac-Sage P, et al. Giant vertebral notochordal rest: a new entity distinct from chordoma. Histopathol. 2005;47(6):646–9.
35. Kreshak J, Larousserie F, Picci P, Boriani S, Mirra J, Merlino B, et al. Difficulty distinguishing benign notochordal cell tumor from chordoma further suggests a link between them. Cancer Imaging. 2014;14(1):1–8.
36. Usher I, Flanagan AM, Choi D. Systematic review of clinical, radiologic, and histologic features of benign notochordal cell tumors: implications for patient management. World Neurosurg. 2019;130:13–23.
37. Kyriakos M, Totty WG, Lenke LG. Giant vertebral notochordal rest: a lesion distinct from chordoma: discussion of an evolving concept. Am J Surg Pathol. 2003;27(3):396–406.
38. Walcott BP, Nahed BV, Mohyeldin A, Coumans JV, Kahle KT, Ferreira MJ. Chordoma: current concepts, management, and future directions. Lancet Oncol. 2012;13(2):e69-76.
39. Rosenthal DI, Scott JA, Mankin HJ, Wismer Gl, Brady TJ. Sacrococcygeal chordoma: magnetic resonance imaging and computed tomography. AJR Am J Roentgenol. 1985;145(1):143–147.
40. Firooznia H, Golimbu C, Raffi N, Reede DL, Kricheff II, Bjorkengren A. Computed tomography of spinal chordomas. J Comput Tomogr. 1986;10(1):45–50.
41. De Bruine FT, Kroon HM. Spinal chordoma: radiologic features in 14 cases. AJR Am J Roentgenol. 1985;150(4):861–3.
42. Meyer JE, Lepke RA, Lindfors KK, Pagani JJ, Hirschy JC, Hayman LA, et al. Chordomas: their CT appearance in the cervical, thoracic and lumbar spine. Radiology. 1984;153(3):693–6.
43. Choi JJ, Murphey MD, Gannon FH, Sweet DS, Jelinek JS. Imaging of chordoma of the spine: radiologic-pathologic correlation. 86th Scientific Assembly and Annual Meeting of the Radiological Society of North America, Chicago, IL, November 27, 2000. 217(P). p. 573.
44. Derlin T, Sohns JM, Hueper K. 68Ga-DOTA-TATE PET/CT for molecular imaging of somatostatin receptor expression in metastasizing chordoma: comparison with 18F-FDG. Clin Nucl Med. 2017;42(4):e210–1.
45. Zhang H, Yoshikawa K, Tanura K, Sagou K, Tian M, Suhara T, et al. Carbon-11-methionine positron emission tomography imaging of chordoma. Skelet Radiol. 2004;33(9):524–30.
46. Sung MS, Lee GK, Kang HS, Kwon ST, Park JG, Suh JS, et al. Sacrococcygeal chordoma: MR imaging in 30 patients. Skelet Radiol. 2005;34(2):87–94.
47. Olson JT, Wenger DE, Rose PS, Petersen IA, Broski SM. Chordoma: 18F-FDG PET/CT and MRI imaging features. Skelet Radiol. 2021;50(8):1657–66.
48. Chhaya S, White LM, Kandel R, Wunder JS, Ferguson P, Agur A. Transarticular invasion of bone tumours across the sacroiliac joint. Skelet Radiol. 2005;34(12):771–7.
49. Llauger J, Palmer J, Amores S, Bagué S, Camins A. Primary tumors of the sacrum: diagnostic imaging. AJR Am J Roentgenol. 2000;174(2):417–24.
50. Major NM, Helms CA, Richardson WJ. The "mini brain": plasmacytoma in a vertebral body on MR imaging. AJR Am J Roentgenol. 2000 [cited 2022 Mar 7];175(1):261–263. Available from https://pubmed.ncbi.nlm.nih.gov/10882284/. https://doi.org/10.2214/ajr.175.1.1750261.
51. Kerekes D, Goodwin CR, Ahmed AK, Verlaan JJ, Bettegowda C, Abu-Bonsrah N, et al. Local and distant recurrence in resected sacral chordomas: a systematic review and pooled cohort analysis. Glob Spine J. 2019;9(2):191–201.
52. Ailon T, Torabi R, Fisher CG, Rhines LD, Clarke MJ, Bettegowda C, et al. Management of locally recurrent chordoma of the mobile spine and sacrum: a systematic review. Spine. 2016;41(Suppl 20):S193–8.
53. Yeom KW, Lober RM, Mobley BC, Harsh G, Vogel H, Allagio R, Pearson M, Edwards MS, Fischbein NJ. Diffusion-weighted MRI: distinction of skull base chordoma from chondrosarcoma. AJNR Am J Neuroradiol. 2013;34(5):1056–1061, S1.
54. Pasalic D, Luetmer PH, Hunt CH, Rose PS, Diehn FE, Folpe AL, Wenger DE. Benign notochordal cell tumor of the sacrum with atypical imaging features: the value of CT guided biopsy for diagnosis. Open Neuroimag J. 2013;7:36–40.
55. Dea N, Fisher CG, Reynolds JJ, Schwab JH, Rhines LD, Gokaslan ZL, et al. Current treatment strategy for newly diagnosed chordoma of the mobile spine and sacrum: results of an international survey. J Neurosurg Spine. 2018;30(1):119–25.
56. Fuchs B, Dickey ID, Yaszemski MJ, Inwards CY, Sim FH. Operative management of sacral chordoma. J Bone Joint Surg Am. 2005;87(10):2211–6.
57. Sciubba DM, Chi JH, Rhines LD, Gokaslan ZL. Chordoma of the spinal column. Neurosurg Clin N Am. 2008;19(1):5–15.
58. Hulen CA, Temple HT, Fox WP, Sama AA, Green BA, Eismont FJ. Oncologic and functional outcome following sacrectomy for sacral chordoma. J Bone Joint Surg Am. 2006;88(7):1532–9.
59. Zuckerman SL, Lee SH, Chang GJ, Walsh GL, Mehran RJ, Gokaslan ZL, et al. Outcomes of surgery for sacral chordoma and impact of complications: a report of 50 consecutive patients with long-term follow-up. Glob Spine J. 2021;11(5):740–50.
60. Pennington Z, Ehresman J, McCarthy EF, Ahmed AK, Pittman PD, Lubelski D, et al. Chordoma of the sacrum and mobile spine: a narrative review. Spine J. 2021;21(3):500–17.
61. Court C, Briand S, Mir O, Le Péchoux C, Lazure T, Missenard G, et al. Management of chordoma of the sacrum and mobile spine. Orthos Traum: Surg Res. 2021;7: 103169.

62. Varga PP, Szövérfi Z, Fisher CG, Boriani S, Gokaslan ZL, Dekutoski MB, et al. Surgical treatment of sacral chordoma: prognostic variables for local recurrence and overall survival. Euro Spine J. 2015;24(5):1092–101.
63. Barber SM, Sadrameli SS, Lee JJ, Fridley JS, Teh BS, Oyelese AA, et al. Chordoma—current understanding and modern treatment paradigms. J Clin Med. 2021;10(5):1054.
64. DeLaney TF, Liebsch NJ, Pedlow FX, Adams J, Weyman EA, Yeap BY, et al. Long-term results of phase II study of high dose photon/proton radiotherapy in the management of spine chordomas, chondrosarcomas, and other sarcomas. J Surg Oncol. 2014;110(2):115–22.
65. Angelini A, Pala E, Calabrò T, Maraldi M, Ruggieri P. Prognostic factors in surgical resection of sacral chordoma. J Surg Oncol. 2015;112(4):344–51.
66. Ji T, Guo W, Yang R, Tang X, Wang Y, Huang L. What are the conditional survival and functional outcomes after surgical treatment of 115 patients with sacral chordoma? Clin Orthop Relat Res. 2017;475(3):620–30.
67. Radaelli S, Stacchiotti S, Ruggieri P, Donati D, Casali PG, Palmerini E, et al. Sacral chordoma: long-term outcome of a large series of patients surgically treated at two reference centers. Spine. 2016;41(12):1049–57.
68. Kayani B, Sewell MD, Tan KA, Hanna SA, Williams R, Pollock R, et al. Prognostic factors in the operative management of sacral chordomas. World Neurosurg. 2015;84(5):1354–61.
69. Pennington Z, Ehresman J, Elsamadicy AA, Shin JH, Goodwin CR, Schwab JH, Sciubba DM. Systematic review of charged-particle therapy for chordomas and sarcomas of the mobile spine and sacrum. Neurosurg foc. 2021;50(5):E17.
70. Akinduro OO, Garcia DP, Domingo RA, Vivas-Buitrago T, Sousa-Pinto B, Bydon M, et al. Cervical chordomas: multicenter case series and meta-analysis. J Neuro Oncol. 2021;153(1):65–77.
71. Boriani S, Bandiera S, Biagini R, Bacchini P, Boriani L, Cappuccio M, et al. Chordoma of the mobile spine: fifty years of experience. Spine. 2006;31(4):493–503.
72. Ahmed R, Sheybani A, Menezes AH, Buatti JM, Hitchon PW. Disease outcomes for skull base and spinal chordomas: a single center experience. Clin Neurol Neurosurg. 2015;130:67–73.
73. Huang JF, Chen D, Zheng XQ, Lin JL, Wang XY, Wu AM. Conditional survival and changing risk profile in patients with chordoma: a population-based longitudinal cohort study. J Orthop Surg Res. 2019;14(1):1–8.
74. Bakker SH, Jacobs WC, Pondaag W, Gelderblom H, Nout RA, Dijkstra PDS, et al. Chordoma: a systematic review of the epidemiology and clinical prognostic factors predicting progression-free and overall survival. Euro Spine J. 2018;27(12):3043–58.
75. Young VA, Curtis KM, Temple HT, Eismont FJ, DeLaney TF, Hornicek FJ. Characteristics and patterns of metastatic disease from chordoma. BioMed Res Intern. 2015 [cited 2022 Mar 7]2015; 7 p. Available from: https://www.hindawi.com/journals/sarcoma/2015/517657/. https://doi.org/10.1155/2015/517657.